Universal distribution of threshold forces at the depinning transition

Andrei A. Fedorenko, Pierre Le Doussal, and Kay Jörg Wiese
CNRS–Laboratoire de Physique Théorique de l'Ecole Normale Supérieure, 24 rue Lhomond, 75231 Paris Cedex, France
(Received 10 July 2006; published 13 October 2006)

We study the distribution of threshold forces at the depinning transition for an elastic system of finite size, driven by an external force in a disordered medium at zero temperature. Using the functional renormalization group technique, we compute the distribution of pinning forces in the quasistatic limit. This distribution is universal up to two parameters, the average critical force and its width. We discuss possible definitions for threshold forces in finite-size samples. We show how our results compare to the distribution of the latter computed recently within a numerical simulation of the so-called critical configuration.

DOI: 10.1103/PhysRevE.74.041110 PACS number(s): 64.60.Ak, 75.60.Ch, 74.25.Qt

I. INTRODUCTION

The dynamics of elastic objects driven by an external force in disordered media has attracted considerable theoretical and experimental interest during recent years [1–3]. The reason is twofold. On one hand, elastic objects in disordered media exhibit the rich behavior of glassy systems and thus their study can help us to understand the physics of more complex systems such as spin glasses [4] or random field systems [5]. On the other hand, the motion of elastic objects in disordered media is an adequate description of many experimental systems. One can divide these systems into two classes. The first class comprises periodic systems, the most prominent examples being charge-density waves (CDW) in solids. These start sliding when the applied electric field becomes large enough [6]. Vortex lines in disordered superconductors form a quasiordered periodic Bragg glass phase [7,8]. The second class includes propagating interfaces such as domain walls in magnetically or structurally ordered systems [9], interfaces between immiscible fluids in porous media [10] or dislocation lines in metals [11]. To unify the mathematical description of these different systems one uses the notion of "manifolds." In all these systems the interplay between quenched disorder and elasticity leads to a complicated response of the system to an applied external force. At zero temperature, a driving force f exceeding a certain threshold value f_c is required to set the elastic manifold into motion. This depinning transition shares many features with critical phenomena [12]: characteristic lengths diverge close to the transition as $\xi \sim (f-f_c)^{-\nu}$ and the system becomes extremely sensitive to small perturbations. Following the description of standard critical phenomena, one can identify the ordered phase with the moving phase with force $f>f_c$, and the order parameter with the velocity v, which vanishes as $v \sim (f-f_c)^{\beta}$ at the transition. One also introduces the dynamic exponent z, which relates time and space by $t \sim x^z$. The critical force f_c, which must be tuned to reach the scale-invariant regime, plays a role similar to the critical temperature in thermal phase transitions. There are many subtleties however, within this analogy, since depinning is a nonequilibrium transition at zero temperature, where quenched disorder dominates. As the corresponding static problem of elastic manifolds in disordered media [13], the depinning problem suffers from two peculiarities when compared to standard critical phenomena: First, an infinite set of operators becomes relevant simultaneously, below the internal upper critical dimension $d<d_{\mathrm{uc}}=4$. Second, their study is more difficult due to the dimensional reduction phenomenon, which renders naive zero-temperature perturbation theory trivial, hence useless. The way out involves first parametrizing the set of relevant operators into a function, $\Delta(u)$, the second cumulant of the random pinning force. It was shown in Refs. [14,15] that the corresponding functional renormalization group (FRG) provides an adequate description of the depinning transition if one considers the nonanalytic renormalized function $\Delta(u)$. It was shown only recently that the FRG can be unambiguously extended to higher loop order and that the underlying nonanalytic field theory is renormalizable [16,17]. The FRG equation for $\Delta(u)$ has two main nontrivial stable fixed points, which describe periodic and interface universality classes. Both of them exhibit a cusp singularity of the form $\Delta^*(u)-\Delta^*(0) \sim |u|$ at small u. This cusp accounts for the existence of the critical threshold force $f_c \sim \Delta^{*\prime}(0^+)$. The corresponding critical exponents have been computed to second order in $\varepsilon=4-d$ [16,17].

Despite this progress many open questions remain. Among them is the problem of sample-to-sample fluctuations, i.e., the probability distributions of a given observable and their relation to extreme value statistics. These were studied mostly for static quantities. The distribution of the energy of pinned manifolds was analyzed in Refs. [18,19]. The distribution of the mean squared width of an interface at the depinning transition was calculated using a Gaussian approximation for the displacement field, yielding a result quite close to numerics [20]. It was shown how systematic corrections can be computed in the field theory of depinning within an $\varepsilon=4-d$ expansion [21]. One expects sample-to-sample fluctuations to play an important role in the dynamics too, leading to a broad distribution of time scales. The divergence of the typical energy barrier with scale, responsible for the ultraslow creep motion, is predicted by phenomenological arguments [7]. A numerical study in Ref. [22] of the distribution of barriers confirms that the typical barrier scales as the energy minima, as predicted by one-loop FRG studies [23]. The more difficult question of predicting the distribution of energy barriers was addressed in Ref. [24] using the FRG, and in Ref. [25] using extreme value statistics.

An important and debated question is to characterize the finite-size fluctuations of the critical force and whether they

obey finite-size scaling (FSS). Similar questions were investigated recently in the context of heteropolymer unbinding transitions (the role of critical force being played there by critical temperature) where violation of FSS was found [26]. In the depinning problem, one difficulty is to define properly the critical force and its fluctuations in the limit of large interface (internal) size L. A recent and efficient algorithm [27] allows us to obtain exactly the critical force f_c of an interface in a periodic medium of period M (i.e., a cylinder), as well as the so-called critical configuration. The latter is defined as the last blocking configuration as f is increased up to f_c, which also defines $f_c=f_c(L,M)$. One can refer to this definition as an extremal configuration in a given sample. The finite-size sample-to-sample distribution of $f_c(L,M)$ was computed numerically [28] and found to depend on the aspect ratio $k=M/L^{\zeta}$ of the cylinder. This should be expected since for large k one recovers a zero-dimensional problem and the interface will be blocked by rare disorder configurations, hence dominated by extremal statistics. However, this result seems to depend on the precise definition and one may ask whether a more fundamental definition exists, with no need to specify a value for k. An alternative approach is to define the observables at the depinning transition as the time average in the moving state at fixed velocity v, in the limit $v \to 0^+$. This definition, to which we refer as the quasistatic depinning limit, is usually associated to the FRG approach of the depinning transition. Observables calculated in this approach must, *a priori*, be distinguished from those computed in the critical configuration. Since the time average is usually performed in a steady state, to avoid dominance by history dependence, it also requires specifying boundary conditions. It is widely believed that both approaches give the same result, at least for ($N=1$ component) interfaces, since in the limit of infinite systems ($L \to \infty$) all quasistatic configurations should have the same statistical properties and the critical force f_c should be self-averaging. However, it is less clear how these approaches compare when applied to finite-size fluctuations where the dispersion in local pinning forces becomes important.

In the present paper we study the distribution of the threshold forces by means of the functional renormalization group. Within the field theory we propose two definitions of the critical force $f_c(L)$ in finite size L and show that they are identical to one loop in the renormalized theory. We compute the cumulants of $f_c(L)$ and extract the distribution, which is found to be universal, up to a shift in f (the critcal force f_c) and one scale parameter (the width of the distribution). All results are valid within the $\varepsilon=4-d$ expansion and extrapolations to low dimension are discussed. The critical force studied here is defined from a fixed center-of-mass ensemble. As we point out it can be, in principle, obtained in numerics. Since it does not refer to any transverse size M, it is more fundamental than the one used in the numerical studies on a cylinder. We discuss how the latter one can, in principle, be recovered.

The paper is organized as follows. Section II introduces the model and the FRG treatment of the depinning transition. In Sec. III we compute the bare distribution of threshold forces to one-loop order using an improved perturbation theory, and renormalize it for the case of an elastic interface. In Sec. IV we discuss the renormalization for periodic systems. In Sec. V we discuss the relation between the distribution of critical forces in the quasistatic limit and in the critical configuration.

II. MODEL AND FRG DESCRIPTION

Let us consider the motion of a one-component elastic manifold with short-range elasticity. The configuration of the manifold can be described by a scalar displacement field u_{xt}, where x denotes the d-dimensional internal coordinate of the manifold. We study the overdamped dynamics of a manifold in the disordered medium, which obeys the following equation of motion:

$$\eta \partial_t u_{xt} = c\nabla^2 u_{xt} + F(x,u_{xt}) + f, \tag{1}$$

where η is the bare friction and c is the elasticity. The quenched random force $F(x,u)$ can be chosen Gaussian with zero mean and variance

$$\overline{F(x,u)F(x',u')} = \Delta(u-u')\delta^d(x-x'). \tag{2}$$

For periodic systems the function $\Delta(u)$ is periodic, while for interfaces it decays exponentially for large u. In the latter case, in contrast to the statics, at depinning both random bond (RB) and random field (RF) microscopic disorder renormalize to the same fixed point, which has RF characteristics, so that we can restrict ourselves to the latter case. a is the width of the function $\Delta(u)$. To make the problem well defined we imply an UV cutoff at scale Λ^{-1}. We consider a finite system of size L with periodic boundary conditions. The size L serves as an IR cutoff, i.e., it plays the role of the mass in the corresponding field theory. One can easily see that due to the tilt symmetry the elastic constant remains uncorrected to all orders so that we are free to fix $c=1$.

Below, starting in Sec. III we will find it convenient to work in the comoving frame. To that end we shift $u_{xt} \to vt + u_{xt}$, such that $\overline{\langle u_{xt} \rangle}=0$ and $f \to f-\eta v$, where $v = L^{-d}\overline{\langle \int_x \partial_t u_{xt} \rangle}$ is the velocity of the center of mass. Here the angular brackets stand for the average over different initial configurations (since we are studying zero-temperature dynamics) and the overline denotes the average over disorder distribution. We will assume that a steady-state attractor has been reached, hence that averages depend only on time differences and not on a specific choice of initial conditions.

To study the dynamics of an elastic manifold efficiently, we use the formalism of generating functionals. Introducing the response field $\hat{u}_{xt}$ one can compute the average of the observable $A[u_{x,t}]$ over dynamic trajectories with different initial conditions for a particular disorder configuration as follows:

$$\langle A[u_{x,t}] \rangle = \int \mathcal{D}[u]\mathcal{D}[\hat{u}]A[u_{x,t}]e^{-S_F[u,\hat{u}]}. \tag{3}$$

S_F is the action for a particular realization of the disorder (a particular sample). To compute the average of the observables, which explicitly depends on the random force at the position of the manifold, we introduce the source J_{xt} for the

random force F so that the corresponding action reads

$$S_F[u,\hat{u}] = \int_{xt} i\hat{u}_{xt}(\eta\partial_t - \nabla^2)u_{xt} - \int_{xt} i\hat{u}_{xt}\{F(x,u_{xt}) + f_{xt}\} - \int_{xt} J_{xt}F(x,u_{xt}). \tag{4}$$

After averaging over the disorder distribution, any observable that depends on the displacement field and the random force at the position of the manifold can be computed as follows:

$$\overline{\langle A[u_{x,t}]F(x_1,u_{x_1,t_1})\cdots F(x_n,u_{x_n,t_n})\rangle} = \frac{\delta}{\delta J_{x_1,t_1}\cdots\delta J_{x_n,t_n}}\int \mathcal{D}[u]\mathcal{D}[\hat{u}]A[u_{x,t}]e^{-S[u,\hat{u}]}\Big|_{J=0}.$$

$S[u,\hat{u}]$ is the effective action, which can be split into two parts: the free part S_0 being quadratic in fields and the interaction part S_{int} containing all nonlinear terms

$$S_0 = \int_{xt} i\hat{u}_{xt}(\eta\partial_t - \nabla^2)u_{xt} - \int_{xt} i\hat{u}_{xt}f_{xt},$$

$$S_{\text{int}} = -\frac{1}{2}\int_{xtt'} (i\hat{u}_{xt} + J_{xt})\Delta(u_{xt} - u_{xt'})(i\hat{u}_{xt'} + J_{xt'}).$$

Setting $J_{xt}=0$ we recover the action used in Refs. [16,17]. The quadratic part S_0 gives the free response

$$\langle u_{q,t}i\hat{u}_{-q,0}\rangle = R_{q,t} = \frac{\Theta(t)}{\eta}e^{-q^2t/\eta}, \tag{5}$$

while the free correlation function is $C_{q,t}=\langle u_{q,t}u_{-q,0}\rangle=0$ at zero temperature. The split diagrammatics for the perturbation theory in disorder Δ was developed in Refs. [16,17]. It is known that naive perturbation theory—obtained by taking for Δ an analytic function—exhibits the property of dimensional reduction and fails to describe the physics, giving, for example, an incorrect roughness exponent. The physical reason for this is the existence of a large number of metastable states.

Let us briefly sketch the FRG analysis of the system under consideration. Power counting shows that the whole function $\Delta(u)$ becomes relevant below $d_{\text{uc}}=4$ and thus one has to renormalize the whole function. To extract the scaling behavior one has to study the flow of the renormalized function Δ under changing the IR cutoff towards infinity. Various choices for the IR cutoff were discussed in Refs. [16,17]. A convenient choice is to add a small mass m, so that the scaling behavior can be extracted from the effective action $\Gamma[u,\hat{u}]$ of the theory as m decreases to zero. To study the finite-size distribution of threshold forces, we use, as in Ref. [21], the system size L as the natural IR cutoff. Then any integral over momentum q has to be replaced by the sum according to the rule $\int_q \to L^{-d}\Sigma_q$, where the sum runs over all $q=2\pi k/L$, $k\in\mathbb{Z}^d$, $k\neq 0$. Exclusion of the zero mode means that we are working in an ensemble of fixed center of mass, a point further discussed in Sec. V.

Let us define the rescaled disorder as

$$\Delta(u) = \frac{1}{\varepsilon\tilde{I}_1}L^{2\zeta-\varepsilon}\tilde{\Delta}(uL^{-\zeta}), \tag{6}$$

where $I_1=L^{\varepsilon}\tilde{I}_1=\int_q|q|^{-2}$ is the one-loop integral. It was shown in Refs. [14,15] that the FRG equation, i.e., the flow equation for the running disorder correlator, can be written to one-loop order as

$$L\partial_L\tilde{\Delta}(u)|_0 = (\varepsilon-2\zeta)\tilde{\Delta}(u) + \zeta u\tilde{\Delta}'(u) - \frac{1}{2}[[\tilde{\Delta}(u)-\tilde{\Delta}(0)]^2]'', \tag{7}$$

the two-loop flow equation being obtained in Refs. [16,17]. "0" means a derivative at fixed bare quantities. The flow of the correlator is such that $\Delta(u)$ acquires a cusp at the origin $u=0$ at the Larkin scale $L_c\simeq[c^2a^2/\Delta(0)]^{1/\varepsilon}$. Beyond the Larkin scale ($L>L_c$) the renormalized correlator is singular and perturbation theory breaks down. Nevertheless, the flow tends to a nontrivial fixed-point (FP) solution $\tilde{\Delta}^*(u)$ with a new value for the roughness exponent, which controls the large-scale behavior. There are two FPs that describe interfaces and periodic systems, correspondingly. The former FP has $\zeta=\varepsilon/3+O(\varepsilon^2)$, while the latter one has $\zeta=0$ due to periodicity. The renormalization of the mobility gives the value of the dynamic exponent,

$$z = 2 + L\frac{d}{dL}\eta_R\Big|_0 = 2 - \tilde{\Delta}''(0) + O(\tilde{\Delta}^2), \tag{8}$$

where η_R is the renormalized mobility. Other critical exponents can be computed using the scaling relations

$$\nu = \frac{1}{2-\zeta} = \frac{\beta}{z-\zeta}. \tag{9}$$

To renormalize the theory, one needs an additional counterterm for the excess force $f-\eta v$, which comes with an UV divergence $\sim\Lambda^2$. This term is analogous to the critical temperature shift in the φ^4 theory, and gives the critical threshold force f_c^*. It is zero in the bare theory. We expect that in the limit of an infinite system $L\to\infty$, the critical force becomes sample independent if there is the same distribution of disorder in each sample and thus $\lim_{L\to\infty}P_L(f)=\delta(f-f_c^*)$. However, the situation is different for finite systems. According to the general theorem for random systems [29] there exists a finite-size scaling correlation length ξ_{FS}, which characterizes the distribution of the observables in an ensemble of samples and which, in principle, has to be distinguished from the intrinsic correlation length ξ, which enters into correlation functions. Approaching the critical point, the finite-size correlation length diverges similar to the intrinsic correlation length as $\xi_{\text{FS}}\sim|f-f_c|^{-\nu_{\text{FS}}}$. In general, ν_{FS} is different from ν, and satisfies the inequality

$$\nu_{\text{FS}} \geqslant 2/(d+\zeta), \tag{10}$$

where $d+\zeta$ is the effective dimension of the disordered system considered. Thus for an ensemble of samples of linear

size L the width of the distribution of critical forces is characterized by a scale $\xi_{\mathrm{FS}}=L$ and reads

$$\overline{\langle (f_c(L)-f_c^*)^2\rangle} \sim L^{-2/\nu_{\mathrm{FS}}}. \tag{11}$$

For periodic systems $\zeta=0$ and $\nu=1/2$ so that $\nu_{\mathrm{FS}}\neq\nu$ for $d\leqslant 4$. For interfaces it was proposed [15] that $\nu_{\mathrm{FS}}=\nu$. While ν_{FS} satisfies Eq. (10) with the equal sign in one-loop order, at two-loop order the inequality becomes strict. As discussed in Refs. [15,17] this difference is closely related to the stability of the FP, which controls the scaling behavior.

III. DISTRIBUTION OF THRESHOLD FORCES

A. Perturbation theory

Let us show how the critical force distribution can be computed within "improved" perturbation theory. Improved means that we assume the disorder correlator $\Delta(u)$ to be nonanalytic, since for analytic disorder perturbation theory gives a zero-threshold force. Then using FRG we renormalize our result to one-loop order. Effectively, this is a summation of an infinite subset of diagrams. We define the distribution of threshold force as follows:

$$P_L(f_c)=\overline{\left\langle \delta\left(f_c+L^{-d}\int_x F(x,vt+u_{xt})\right)\right\rangle}. \tag{12}$$

From now on we work in the comoving frame and the average is performed with the action S in the quasistatic limit $v\to 0^+$, as is usually done in the FRG theory of the depinning transition.

Let us introduce the corresponding characteristic function

$$\hat{P}_L(\lambda)=\overline{\langle e^{-i\lambda f_c(L)}\rangle}=\int df_c e^{-i\lambda f_c}P_L(f_c), \tag{13}$$

which can be expressed through the cumulants $\overline{\langle f_c(L)^n\rangle}_c$ as follows:

$$\hat{P}_L(\lambda)=\exp\left(\sum_{n=1}^{\infty}\frac{(-i\lambda)^n}{n!}\overline{\langle f_c(L)^n\rangle}_c\right). \tag{14}$$

The computation of the first cumulant to one loop is trivial. The random force that the interface actually feels in the point x is given by

$$\overline{\langle F(x,u_{x,t}+vt)\rangle}=\left\langle\int_{t_1}\Delta[u_{xt}-u_{xt_1}+v(t-t_1)]i\hat{u}_{xt_1}\right\rangle$$
$$=\int_{t_1}\Delta'[v(t-t_1)][R_{x=0,t-t_1}-R_{x=0,t=0}]. \tag{15}$$

We will adopt Ito's prescription in which $R_{x,t=0}=0$. Note that this corresponds to the definition $\Theta(0)=0$. Taking the quasistatic limit $v\to 0^+$, we obtain the well-known expression for the average critical force

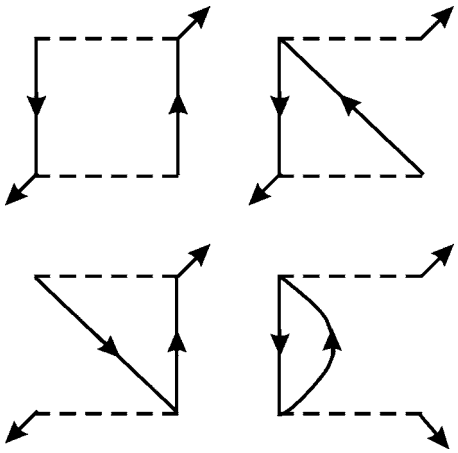

FIG. 1. Diagrams D_i $(i=1,\ldots,4)$ contributing to the second cumulant of the threshold force. We have adopted the split diagrammatics used in Ref. [17]: the arrowed line indicates a response propagator (5); the dashed line indicates the split vertex $i\hat{u}_{xt}i\hat{u}_{xt'}\Delta(u_{xt}-u_{xt'})$. The corresponding expressions are given by Eq. (19).

$$f_c^*=-\Delta'(0^+)\int_0^{\infty}dtR_{x=0,t}=-\int_q\frac{\Delta'(0^+)}{q^2}. \tag{16}$$

Note that the critical force (16) diverges at large momentum as Λ^{d-2} and therefore is not universal, i.e., it depends on microscopic parameters. This is analogous to the shift of the critical temperature in standard critical phenomena, caused by fluctuations. As we know, this shift is also nonuniversal. However, we expect that the distribution of critical forces for a finite system around the average value is universal, once the distribution is properly normalized. The computation of the nth cumulant is more tricky. Before considering the general case, let us show how this works for the second cumulant. Using the generating functional, we can write down the formal expression for the effective force-force correlator,

$$\overline{\langle F(x_1,u_{x_1,t}+vt)F(x_2,u_{x_2,t}+vt)\rangle}$$
$$=\Delta(0)\delta^d(x_1-x_2)+\left\langle\int_{t_1}\Delta[u_{x_1t}-u_{x_1t_1}+v(t-t_1)]i\hat{u}_{x_1t_1}\right.$$
$$\left.\times\int_{t_2}\Delta[u_{x_2t}-u_{x_2t_2}+v(t-t_2)]i\hat{u}_{x_2t_2}\right\rangle. \tag{17}$$

The first term on the right-hand side of Eq. (17) is the bare disorder distribution. It is given by Eq. (2) and is a pure Gaussian distribution with zero mean. However, the moving manifold explores a different distribution, that is an effective distribution, which one can observe "sitting" on the moving interface. The second term on the right-hand side of Eq. (17) as well as the mean value (15) are the deviation of the effective distribution from the bare one. Only connected diagrams contribute to the second cumulant. Integrating the second term in Eq. (17) over fields with the weight e^{-s} we obtain the four connected diagrams shown in Fig. 1. The corresponding expressions can be rewritten as follows:

$$\int_{t_1 t_2} \Delta'[v(t-t_1)][R_{x_2-x_1,t-t_1} - R_{x_2-x_1,t_2-t_1}],$$

$$\Delta'[v(t-t_2)][R_{x_1-x_2,t-t_2} - R_{x_1-x_2,t_1-t_2}]. \tag{18}$$

To compute the contribution to the variance of the critical force, we have to integrate over x_1 and x_2 and then multiply by L^{-2d}. This computation is more convenient in Fourier representation;

$$D_1 + D_2 + D_3 + D_4 = L^{-d}[\Delta'(0^+)]^2 \int_{q t_1 t_2} [R_{q,t-t_1} - R_{q,t_2-t_1}][R_{q,t-t_2} - R_{q,t_1-t_2}]. \tag{19}$$

Due to causality we have $D_4=0$. The other diagrams read

$$D_1 = -D_2 = -D_3 = L^{-d} \int_q \frac{[\Delta'(0^+)]^2}{(q^2)^2}. \tag{20}$$

Summing all contributions we obtain

$$\overline{\langle f_c(L)^2 \rangle}_c = L^{-d}\Delta(0) - L^{-d} \int_q \frac{[\Delta'(0^+)]^2}{(q^2)^2}. \tag{21}$$

We have also derived Eq. (21) by using direct perturbation theory instead of the generating functional.

The above calculation can be generalized to arbitrary n. It can be simplified significantly if one takes into account that all intermediate times t_i must be smaller than the observation time t: $t_i < t$ $(i=1,\ldots,n)$. For the nth cumulant $(n>2)$ we have

$$\overline{\langle f_c(L)^n \rangle}_c = (-1)^n (n-1)! L^{-d(n-1)} \int_q [\Delta'(0^+)]^n \times \int_{t_1 \cdots t_n} [R_{q,t-t_1} - R_{q,t_2-t_1}][R_{q,t-t_2} - R_{q,t_3-t_2}] \cdots \times [R_{q,t-t_{n-1}} - R_{q,t_n-t_{n-1}}][R_{q,t-t_n} - R_{q,t_1-t_n}]. \tag{22}$$

Here the factor $(n-1)!$ results from different contractions of $u_{x_i t} - u_{x_i t_i}$ and $\hat{u}_{x_j t_j}$ $(i,j=1,\ldots,n)$ that form a closed loop. Expanding the integrand in Eq. (22) we find that all terms give the same contribution up to a factor of ± 1, except for the term composed only from the second response function in each bracket. This term gives a closed loop of response functions, which is zero by causality. Using the identity

$$\sum_{i=0}^{n-1} (-1)^i C_n^i = (-1)^{n+1}, \tag{23}$$

where C_n^i is a binomial coefficient, we can simplify Eq. (22) to

$$\overline{\langle f_c(L)^n \rangle}_c = -(n-1)! L^{-d(n-1)} \int_q \frac{[\Delta'(0^+)]^n}{q^{2n}}. \tag{24}$$

We are now in a position to construct the characteristic function

$$\ln \hat{P}(\lambda) = -\frac{1}{2}\Delta(0) L^{-d} \lambda^2 - L^d \int_q \sum_{n=1}^{\infty} \frac{(-1)^n}{n} \left(\frac{\Delta'(0^+)}{q^2} L^{-d} i\lambda \right)^n. \tag{25}$$

The latter is nothing but the Taylor series of the logarithm, which allows us to rewrite Eq. (25) as

$$\hat{P}(\lambda) = \exp\left[-\frac{1}{2}\Delta(0) L^{-d}\lambda^2 + L^d \int_q \ln\left(1 - \frac{|\Delta'(0^+)|}{q^2} L^{-d} i\lambda \right) \right], \tag{26}$$

where we have taken into account that $\Delta'(0^+) < 0$.

As follows from the above computation, the distribution of the critical force can be related to the effective action $\Gamma[u,\hat{u}]$, which is a generating functional for one-particle irreducible (1PI) vertex functions $\Gamma^{(E,S)}_{\hat{u}\cdots\hat{u};u\cdots u}$ with S external fields u and E external fields $\hat{u}$,

$$\Gamma^{(E,S)}_{\hat{u}\cdots\hat{u};u\cdots u}(\{\hat{q}_i,\hat{\omega}_i\},\{q_j,\omega_j\}) = \prod_{i=1}^{S} \frac{\delta}{\delta u_{q_i,\omega_i}} \prod_{j=1}^{E} \frac{\delta}{\delta \hat{u}_{\hat{q}_j,\hat{\omega}_j}} \Gamma[u,\hat{u}] \Big|_{u=\hat{u}=0}. \tag{27}$$

Indeed, as already seen from the bare action the average threshold force can be expressed as vertex function $\Gamma^{(1,0)}_{\hat{u}}$ $(q=0,\omega=0)$ in the quasistatic limit $v \to 0^+$. Analogously, the higher-order cumulants can be identified as the higher-order vertex functions according to

$$\overline{\langle f_c(L)^n \rangle}_c = L^{-(n-1)d} \Gamma^{(n,0)}_{\hat{u}\cdots\hat{u}}(\{q_i=0,\omega_i=0\}). \tag{28}$$

The general properties of vertex functions (28) for even n was discussed in Ref. [21]. In particular, it was noted that loop diagrams that contribute to the vertex $\Gamma^{(2n,0)}$ precisely cancel each other so that the result is given by minus the missing contribution from acausal loops. It is easy to verify by direct inspection of the Feynman diagrams that definitions (12) and (28) give the same result in the one-loop approximation, but the question of their equivalence to all orders is open.

B. Renormalization

In this section we focus on the interface problem, periodic systems being considered in the next section. The distribution of the critical forces in Eq. (26) has been obtained from the improved perturbation theory, and thus, it cannot be reproduced within the Larkin-type models in which all observables depend only on $\Delta(0)$. However, in the bare theory the disorder correlator is an analytic function so that to make the calculation consistent we have to first renormalize our theory. To that end we replace the bare correlator by the renormalized one. This can be viewed as a partial summation of an infinite series of diagrams. If we want the distribution of f_c strictly to lowest order in $\varepsilon=4-d$, then the work is essentially done. However, we will demand a bit more and take an additional effect into account: replacing the bare correlator by the running one in a particular diagram we have to be careful because the scale dependence acquired by the cor-

relator may be in a form of either dependence on a mass (as in quantities that do not contain integration over momentum) or dependence on the loop momentum (which has to be integrated out), or a combination of both. The final result presented here will thus be exact to lowest order in ε and in addition will contain some effects beyond that order (although a full-fledge two-loop calculation is not attempted here). This will allow us to discuss in the next section some extrapolations to low dimension.

Let us start from the renormalization of the first cumulant, i.e., the average critical force (16). We remind the reader that the average critical force is a nonuniversal quantity and afterwards we will subtract it and consider the shifted distribution, which is a universal function. According to Eq. (6) the renormalized disorder correlator acquires in the vicinity of the fixed point a scale dependence. Integration over scales beyond the Larkin scale yields (see Refs. [23,30] for details)

$$\overline{\langle f_c(L)\rangle}_c \approx -\tilde{\Delta}^{*\prime}(0^+)\frac{\Lambda^{2-\zeta}}{2-\zeta}, \tag{29}$$

where in this formula the UV cutoff Λ is meant to be the minimal length of pinned segments of the manifold, i.e., the Larkin length $\Lambda \sim L_c^{-1}$.

We now consider the renormalization of the second cumulant (variance). The corresponding bare expression can be expressed through the two-point vertex function as follows:

$$\begin{aligned}\overline{\langle f_c(L)^2\rangle}_c &= L^{-d}\left[\Delta(0) - \int_q \frac{\Delta'(0^+)^2}{q^4}\right] + O(\Delta^3) \\ &= L^{-d}\Gamma^{(2,0)}_{\hat{u}\hat{u}}(\omega=0;q=0).\end{aligned} \tag{30}$$

As it was shown in Refs. [17,21], the two-point vertex function does not depend on times and scales,

$$\Gamma^{(2)}_{\hat{u}\hat{u}}(q) = L^{2\zeta-\varepsilon}\frac{1}{\tilde{I}_1\varepsilon}\tilde{\Delta}^*(0)F_2(qL), \tag{31}$$

with $F_2(z)=Bz^{\varepsilon-2\zeta}+O(\ln z/z^2)$ for large z and $F_2(0)=1$. Note the constant B depends on the IR cutoff scheme [21]. Combining Eqs. (30) and (31) we obtain

$$\overline{\langle f_c(L)^2\rangle}_c = L^{2\zeta-4}\frac{1}{\tilde{I}_1\varepsilon}\tilde{\Delta}^*(0). \tag{32}$$

We note that this is consistent with the finite-size scaling prediction

$$\overline{\langle f_c(L)^2\rangle}_c \sim L^{-2/\nu} \tag{33}$$

using $\nu=1/(2-\zeta)$. As we will show below, the full (shifted) distribution is also consistent with this scaling.

To proceed further, let us first consider some typical diagrams contributing to the third cumulant of the critical force, which are shown in Fig. 2. To renormalize them at lowest order, we have replaced the disorder lines by the three-point vertices defined as follows:

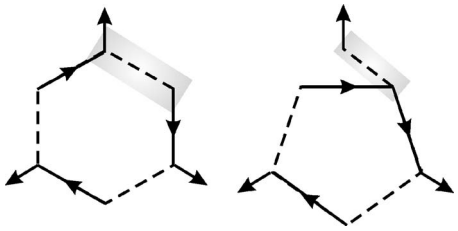

FIG. 2. Example of diagrams contributing to the third cumulant of the critical force. To renormalize these one-loop diagrams to the lowest order we replace the disorder lines by vertices $\Gamma^{(+)}_{\hat{u}\hat{u}u}$ (highlighted on the left diagram) and $\Gamma^{(-)}_{\hat{u}\hat{u}u}$ (highlighted on the right diagram), which are defined in Eqs. (35) and (36) and depicted in detail in Fig. 3.

$$\Gamma^{(2,1)}_{\hat{u}\hat{u}u}(t,t_1,t_2;q_1,q_2) = \Gamma^{(+)}_{\hat{u}\hat{u}u}(t,t_1,t_2;q_1,q_2) + \Gamma^{(-)}_{\hat{u}\hat{u}u}(t,t_1,t_2;q_1,q_2). \tag{34}$$

At tree level, the vertex function (34) can be expressed by diagrams shown in Fig. 3 and the corresponding expressions read

$$\Gamma^{(+)}_{\hat{u}\hat{u}u}(t,t_1,t_2;q_1,q_2) = \Delta'(0^+)\mathrm{sgn}(t-t_1)\delta(t-t_2), \tag{35}$$

$$\Gamma^{(-)}_{\hat{u}\hat{u}u}(t,t_1,t_2;q_1,q_2) = \Delta'(0^+)\mathrm{sgn}(t_1-t)\delta(t_1-t_2). \tag{36}$$

Then the summation of diagrams contributing to the nth cumulant with $n>2$ can be carried out along the lines used for the bare cumulant and gives

$$\begin{aligned}\overline{\langle f_c(L)^n\rangle}_c = (-1)^n(n-1)!L^{-d(n-1)} &\times \int_q \int_{t_1\cdots t_n} \int_{\tau_1\cdots\tau_n} [\Gamma^{(2,1)}_{\hat{u}\hat{u}u}(t,t_2,\tau_1;q,-q)R_{q,\tau_1-t_1}] \\ &\times [\Gamma^{(2,1)}_{\hat{u}\hat{u}u}(t,t_3,\tau_2;q,-q)R_{q,\tau_2-t_2}]\cdots \\ &\times [\Gamma^{(2,1)}_{\hat{u}\hat{u}u}(t,t_n,\tau_{n-1};q,-q)R_{q,\tau_{n-1}-t_{n-1}}] \\ &\times [\Gamma^{(2,1)}_{\hat{u}\hat{u}u}(t,t_1,\tau_n;q,-q)R_{q,\tau_n-t_n}].\end{aligned} \tag{37}$$

Substituting the tree-level expressions (34)–(36) to Eq. (37) we recover the bare cumulant (22).

In the Appendix we compute the vertex function $\Gamma^{(+)}_{\hat{u}\hat{u}u}$ to one-loop order and obtain its large-q asymptotics, which reads

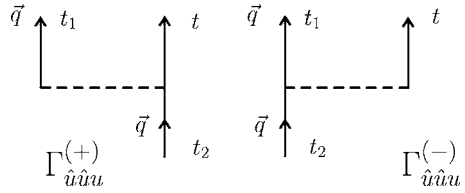

FIG. 3. Vertex function $\Gamma^{(2,1)}_{\hat{u}\hat{u}u}(t,t_1,t_2;q,-q)$ at the tree level. The functions are distinguished by whether the line entering at t_2 and outgoing at t_1 is "closed" $\Gamma^{(-)}_{\hat{u}\hat{u}u}$, or "open" $\Gamma^{(+)}_{\hat{u}\hat{u}u}$. In the first case the time ordering along the loop is continuous: $t_1<t_2$, while in the second case it is interrupted, i.e., there are no restrictions on t_1 and t_2 (see also Fig. 2).

$$\int_{t_2} \Gamma^{(+)}_{\hat{u}\hat{u}u}(t,t_1,t_2;q,-q) = AL^{\zeta-\varepsilon}(qL)^{\psi}, \tag{38}$$

where times t_1 and t are taken infinitely apart (hence it is a quasistatic quantity). The amplitude A and the exponent ψ are given by

$$A = \frac{1}{\varepsilon \tilde{I}_1} \tilde{\Delta}'^{*}(0^+)[1 + O(\varepsilon)], \tag{39}$$

$$\psi = \frac{4}{9}\varepsilon + O(\varepsilon^2), \tag{40}$$

and we argue that ψ is a new exponent (see the Appendix). Taking into account this momentum dependence in Eq. (37) should result in an improved renormalization scheme (compared to simply replacing the bare quantities by q-independent but scale-dependent renormalized parameters) with a different form for the q summations appearing below.

After substituting Eq. (38) in Eq. (34), the integration over times can be performed in the same way as for the bare cumulant and gives for $n>2$ [31]

$$\overline{\langle f_c(L)^n \rangle}_c = -(n-1)! A^n L^{n(\zeta-2)} L^d \int_q \frac{1}{(qL)^{n(2-\psi)}}. \tag{41}$$

Note that $A \sim \tilde{\Delta}^{*\prime}(0^+) < 0$. To construct the characteristic function let us redefine $\lambda \to (2\pi)^{2-\psi}\lambda/(|A|L^{\zeta-2})$, which corresponds to measuring f_c in units of $|A|L^{\zeta-2}/(2\pi)^{2-\psi}$. This is a nonuniversal scale as the value of $\tilde{\Delta}^{*\prime}(0^+)$ is not universal at the depinning transition. However as we now show, once rescaled the (shifted) distribution is universal.

The characteristic function can be written as

$$\ln \hat{P}(\lambda) = -\frac{1}{2}\sigma^2\lambda^2 - \sum_{\mathbf{k}\in Z^d,\mathbf{k}\neq 0} \sum_{n=3}^{\infty} \frac{1}{n}\left(\frac{i\lambda}{|\mathbf{k}|^{2-\psi}}\right)^n, \tag{42}$$

where

$$\sigma^2 = \frac{(2\pi)^4 \tilde{\Delta}^{*}(0)}{A^2 \tilde{I}_1 \varepsilon} = \varepsilon \tilde{I}_1 \frac{\tilde{\Delta}^{*}(0)}{[\tilde{\Delta}'^{*}(0)]^2}(2\pi)^{4-2\psi} = \frac{6\pi^2}{\varepsilon}[1 + O(\varepsilon)]. \tag{43}$$

To compute this universal ratio to lowest order in ε we have used the one-loop FRG fixed-point equation evaluated at $u=0$, i.e., $(\varepsilon-2\zeta)\tilde{\Delta}^{*}(0) = \tilde{\Delta}^{*\prime}(0^+)^2$ and used $\zeta = \varepsilon/3 + O(\varepsilon^2)$, as well as $\varepsilon \tilde{I}_1 = 1/(8\pi^2) + O(\varepsilon)$. Summing over n we obtain

$$\ln \hat{P}(\lambda) = -\frac{1}{2}\sigma^2\lambda^2 + \sum_{\mathbf{k}\in Z^d,\mathbf{k}\neq 0} \left[i\lambda \frac{1}{|\mathbf{k}|^{2-\psi}} - \frac{1}{2}\lambda^2 \frac{1}{|\mathbf{k}|^{2(2-\psi)}} + \ln\left(1 - \frac{i\lambda}{|\mathbf{k}|^{2-\psi}}\right)\right]. \tag{44}$$

C. Lowest order in $\varepsilon = 4-d$

To obtain the distribution within the ε expansion it is sufficient to set $\psi=0$ in the formula above, and to compute all sums in $d=4$. Let us first give the skewness and kurtosis to lowest order in the ε expansion. One uses [21]

$$\sum_{\mathbf{k}\in Z^d,\mathbf{k}\neq 0} \frac{1}{|\mathbf{k}|^{2p}} = \frac{1}{(p-1)!}\int_0^{\infty} dt\, t^{p-1}[\Theta(3,0,e^{-t})^d - 1], \tag{45}$$

$$\sum_{\mathbf{k}\in Z^4,\mathbf{k}\neq 0} \frac{1}{|\mathbf{k}|^6} = 14.8298, \tag{46}$$

$$\sum_{\mathbf{k}\in Z^4,\mathbf{k}\neq 0} \frac{1}{|\mathbf{k}|^8} = 10.2454, \tag{47}$$

where $\Theta(3,0,e^{-t}) = \Sigma_{k\in Z} e^{-tk^2}$ is the elliptic theta function. Hence

$$\sigma_3 = \frac{\overline{(f-\bar{f})^3}}{\sigma^3} = \frac{2}{\sigma^3} \sum_{\mathbf{k}\in Z^d,\mathbf{k}\neq 0} \frac{1}{|\mathbf{k}|^6} \tag{48}$$

$$= 0.0650861\varepsilon^{3/2}, \tag{49}$$

$$\sigma_4 = \frac{\overline{(f-\bar{f})^4}}{\sigma^4} - 3 = -\frac{3!}{\sigma^4} \sum_{\mathbf{k}\in Z^4,\mathbf{k}\neq 0} \frac{1}{|\mathbf{k}|^8} \tag{50}$$

$$= -0.01753\varepsilon^2. \tag{51}$$

Next one can resum to obtain the characteristic function to lowest order in ε;

$$\ln \hat{P}(\lambda) = -\frac{1}{2}\sigma^2\lambda^2 - F(-i\lambda), \tag{52}$$

$$F(-i\lambda) = \int_0^{\infty} \frac{dt}{t}\left(e^{i\lambda t} - 1 - i\lambda t + \frac{1}{2}\lambda^2 t^2\right)[\Theta(3,0,e^{-t})^4 - 1]. \tag{53}$$

This result can be reexpressed as follows. As $d \to 4^-$ the shifted dimensionless critical force

$$\tilde{f} = [f_c(L) - \overline{f_c(L)}]/\sqrt{\overline{f_c(L)^{2c}}}$$

becomes a univariate Gaussian random variable. For small $\varepsilon > 0$, $\tilde{f}$ can be (formally) expressed as the sum of two independent random variables $\tilde{f} = f_0 + \frac{\sqrt{\varepsilon}}{\sqrt{6}\pi} f_1$ where f_0 is a Gaussian of variance $1+O(\varepsilon)$ and f_1 is a random variable of order unity with a nontrivial distribution, the logarithm of its characteristic function being given (up to a quadratic term) by $F(-i\lambda)$.

We now analyze the shape of these distributions in physical dimension.

D. Fourier inversion

In this section we compute the inverse Fourier transform of Eq. (44) in physical dimensions, using our improved scheme.

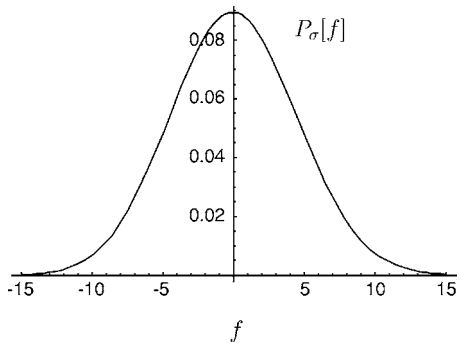

FIG. 4. The three indistinguishable curves for shifted critical-force distribution ($d=1$): improved perturbation theory ($\psi=0$), renormalized to one-loop theory and approximate expression (56). Here $\sigma=\pi\sqrt{2}$. The difference between distributions is shown in Fig. 5.

Let us start by discussing $d=1$. We use a natural extrapolation of our above result, setting $\varepsilon=3$ in the above formulas (which are exact to lowest order in ε). From Eq. (44) we obtain

$$\hat{P}(\lambda) = \exp[-\pi^2\lambda^2]\prod_{k=1}^{\infty}\left\{\left(1-\frac{i\lambda}{k^{2/3}}\right)^2 \exp\left[i\lambda\frac{2}{k^{2/3}} - \lambda^2\frac{1}{k^{4/3}}\right]\right\}, \tag{54}$$

where we have used $\psi=4/3$ and $\sigma=\pi\sqrt{2}$. The inverse Fourier transform computed numerically is shown in Fig. 4. Equation (44) with $\psi=0$ can formally be considered as the result of improved perturbation theory in nonanalytic disorder. The inverse Fourier transform of the latter is also shown in Fig. 4 and cannot be visually distinguished from the shifted renormalized distribution. The renormalized distribution is more appealing since it guarantees a non-negative defined critical force, which is not the case for the bare one, especially in $d=1$ where the bare averaged critical force (16) is finite. By contrast the averaged renormalized critical force is controlled by the UV cutoff and is of order $L_c^{-1/\nu}$ while the typical fluctuation is much smaller, of order $L^{-1/\nu}$, in the limit of interest, here $L \gg L_c$. It is interesting that the renormalized distribution is well approximated by Eq. (54) in which we keep only the first factor with $k=1$;

$$\hat{P}(\lambda) \approx \exp\left[-\frac{1}{2}\sigma^2\lambda^2\right]\{(1-i\lambda)^2\exp[2i\lambda-\lambda^2]\}. \tag{55}$$

The inverse Fourier transform of Eq. (55) reads

$$P[f] \approx \frac{[(\sigma^2+f+4)^2-2-\sigma^2]}{(2+\sigma^2)^{5/2}\sqrt{2\pi}} e^{-[(2+f)^2/2(2+\sigma^2)]} \tag{56}$$

and is also shown in Fig. 4. The difference in the critical-force distributions obtained within improved perturbation theory, renormalized to one-loop theory and approximation (56), is indicated in Fig. 5.

For a d-dimensional system the Fourier transform of the critical-force distribution (44) can be written as

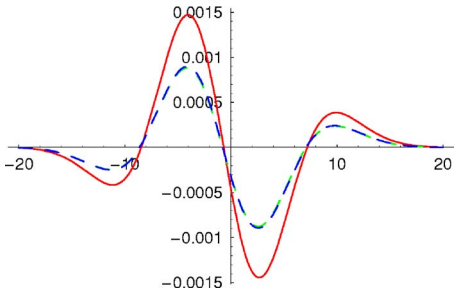

FIG. 5. (Color online) Shifted critical-force distribution for $d=1$ with the Gaussian subtracted. The dashed lines: approximate expression (56) and improved perturbation theory ($\psi=0$); solid line: renormalized to one-loop theory.

$$\hat{P}(\lambda) = \exp\left[-\frac{1}{2}\sigma^2\lambda^2\right]\prod_{\mathbf{k}\in Z^d,\mathbf{k}\neq 0}\left\{\left(1-\frac{i\lambda}{|\mathbf{k}|^{2-\psi}}\right)\right.$$
$$\left.\times\exp\left[i\lambda\frac{1}{|\mathbf{k}|^{2-\psi}} - \frac{1}{2}\lambda^2\frac{1}{|\mathbf{k}|^{2(2-\psi)}}\right]\right\}. \tag{57}$$

Analogously to the case $d=1$ the inverse Fourier transform of Eq. (57) can be well approximated by

$$\hat{P}(\lambda) = \exp\left[-\frac{1}{2}\sigma^2\lambda^2\right]\{(1-i\lambda)^{2d}\exp[2di\lambda - d\lambda^2]\}, \tag{58}$$

which does not depend on ψ.

We now compute the standard deviation and the kurtosis of the above distributions. The standard deviation reads

$$\overline{(f-\bar{f})^2} \equiv \sigma^2. \tag{59}$$

The skewness is defined as

$$\sigma_3 = \frac{\overline{(f-\bar{f})^3}}{\sigma^3} = \frac{2}{\sigma^3}\sum_{\mathbf{k}\in Z^d,\mathbf{k}\neq 0}\frac{1}{|\mathbf{k}|^{3(2-\psi)}}. \tag{60}$$

For $d=1$ we obtain $\sigma_3=\sqrt{2}/(6\pi)\simeq 0.075$ [0.046 for the distribution (56)]. The positive value for the skewness indicates that the right tail of the distribution is heavier than the left tail.

The kurtosis for a Gaussian distribution is three. For this reason, excess kurtosis is defined as

$$\sigma_4 = \frac{\overline{(f-\bar{f})^4}}{\sigma^4} - 3 = -\frac{3!}{\sigma^3}\sum_{\mathbf{k}\in Z^d,\mathbf{k}\neq 0}\frac{1}{|\mathbf{k}|^{4(2-\psi)}}. \tag{61}$$

For $d=1$ we obtain $\sigma_4=-3\zeta(8/3)/\pi^4\simeq -0.04$ [-0.031 for the distribution (56)]. Here $\zeta(x)$ is the Riemann zeta function. The small negative excess kurtosis indicates that the distribution is slightly more flat than a Gaussian distribution, while the deviation from the Gaussian distribution is quite small.

IV. PERIODIC SYSTEMS

The renormalization of the critical-force distribution for periodic systems requires a separate consideration. Indeed as

was shown in Ref. [15], in the periodic case there is an additional relevant operator, which is the uniform part of $\Delta(u)$ so that the random periodic (RP) fixed point is unstable. The flow equation for this operator can be derived by the integration of the renormalization group. (RG) equation over one period [17]

$$L\partial_L \int_0^1 \tilde{\Delta}(u)du = \varepsilon \int_0^1 \tilde{\Delta}(u)du + O(\Delta^3), \tag{62}$$

where we have explicitly used $\zeta=0$. Thus in the vicinity of the RP FP, the flow of the dimensionless disorder is given by

$$\tilde{\Delta}(u) = \tilde{\Delta}^*(u) + cL^{\varepsilon}, \tag{63}$$

where the nonuniversal constant c can be estimated as [17]

$$\begin{aligned} c &= L_c^{-\varepsilon} \int_0^1 [\tilde{\Delta}^{(\text{bare})}(u) - \tilde{\Delta}^*(u)]du \\ &= -L_c^{-\varepsilon} \int_0^1 \tilde{\Delta}^*(u)du \\ &= L_c^{-\varepsilon}\left(\frac{\varepsilon^2}{108} + O(\varepsilon)\right) > 0. \end{aligned}$$

This runaway correction to the scaling behavior at the RP FP contributes to all quantities that depend on $\Delta(0)$ but not to those that depend on $\Delta'(0)$. Therefore in the case of a periodic system the renormalized second cumulant of the critical force reads

$$\overline{\langle f_c(L)^2\rangle_c} = \frac{1}{\tilde{I}_1 \varepsilon}\tilde{\Delta}^*(0)L^{-4} + \frac{c}{\tilde{I}_1 \varepsilon}L^{-d}. \tag{64}$$

Higher-order cumulants are still given by Eq. (41) with $\zeta=0$ and therefore scale with L as $\overline{\langle f_c(L)^n\rangle_c} = L^{-2n}$. We would like to emphasize that the correction to scaling in Eq. (64) describes the sample-to-sample fluctuations and cannot be seen in one sample because in each sample there is only one pinned configuration. As a result, for $d<4$ only the second cumulant of the *scaled* critical force, which scales as L^{-d}, survives in the limit $L\to\infty$ resulting in $\nu_{\text{FS}}=2/d$ and a pure Gaussian distribution for the scaled critical force.

V. DISCUSSION

In the present paper we have computed the renormalized distribution $P[f-\eta v]$ averaged over all pinned configurations in the limit $v\to 0^+$, which we identify with the critical-force distribution $P_L(f_c)$. The average critical force is a nonuniversal quantity, which depends on microscopic details of the interactions like the UV cutoff as well as on details of the disorder distribution. After subtraction of the average value, the shifted distribution of the critical force contains only one nonuniversal scale, which can be fixed, e.g., by fixing the second cumulant. The resulting dimensionless distribution is then fully universal, i.e., it does not depend on properties at small scales. We have computed it taking into account only the second cumulant of the bare disorder distribution, since it is the only cumulant relevant in the RG sense. Higher cumulants, which are generated by coarse graining are irrelevant operators and their contribution to the cumulants of the critical force must carry additional dependence on the cutoff. Hence we expect that they result only in a shift of the nonuniversal expectation values.

Let us now discuss the role of the transverse sample size M (size of the box). In numerical studies of depinning of elastic interfaces, either via an exact determination of the critical state or via Langevin dynamics [20,27,28,32,33] a cylindrical system, which is periodic in both directions, was studied: longitudinal with period L and transverse with period M. Hence this is equivalent to a periodic disorder with period M. It is known that a periodic system has a unique pinned configuration for any period M [34]. If $M \ll L$, this configuration spreads out through the whole box $L^d \times M$ and there is only one independent pinned configuration. As we have shown for the RP class the distribution of critical forces is Gaussian, and thus, for elastic interfaces in the limit $L\to\infty$ with M fixed, the distribution of the critical force also becomes Gaussian.

The case where the period M is taken to infinity at the same time as L is relevant for elastic interfaces and quite different. The pinned interface has a rms width $w=k_w L^{\zeta}$ so that in a sample of transverse size w it also has one unique statistically independent pinned configuration. One may then argue that its critical-force distribution is $P_L(f_c)$ whose characteristic function is given by Eq. (44). In the numerical studies one should thus be careful in choosing the size of the periodic box M. If M scales like $L^{\zeta'}$ with $\zeta'<\zeta$ the system will cross over from the random manifold to the RP FP and the finite-size scaling analysis will result in some mixture of interface and periodic system properties, while the critical-force distribution will tend to a Gaussian one. On the other hand, if $M \gg w$, the sample can be divided into about M/w subsamples, which can be argued to be (almost) statistically independent, with independent pinned configurations. Each configuration has a slightly different critical force, which is distributed according to our FRG result. If one defines the total critical force as a maximum of all the critical forces of these subsamples, it becomes M dependent and its shifted distribution tends to the distribution of the extreme value statistics [28]. Following Ref. [28] let us introduce for every configuration α of the interface in the sample of width $M=kL^{\zeta}$ the depinning force $f_d(\alpha)$ and then associate the threshold force of the whole sample with the following maximal value $f_c^r=\max_{\alpha}\{f_d(\alpha)\}$. In each sample there are only $\approx M/w$ independent pinned configurations, so that the distribution of the maximum of the corresponding critical forces can be written as

$$P_M(f_c^r, M/w) = \frac{d}{df_c^r}\left[\int_{-\infty}^{f_c^r} df' P_L[f'],\right]^{M/w}. \tag{65}$$

According to the general theorem of extreme value statistics [35], for large samples, i.e., in the limit $M/w\to\infty$ this distribution approaches the Gumbel distribution. The latter is provided by the *tails* of the distribution of the critical force for each independent pinning configuration, as given in Eq. (44).

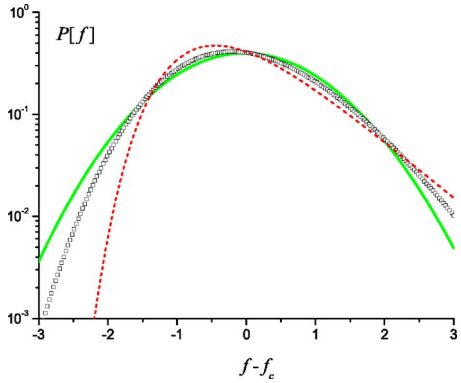

FIG. 6. (Color online) The normalized critical-force distribution for $d=1$. The solid line is the distribution for the interface in the box of size w given by Eq. (56). The dashed line is the Gumbel distribution, i.e., the distribution of the maximal threshold force in the limit of an infinite box. The points are computed using Eq. (65) for the interface in the finite box of size $M=10w$.

According to this distribution the average maximal threshold force of samples of size M behaves as $\ln(k/k_w)$. For large samples with $M \gg w$ it can be extremely large. The above procedure completely washes out all details of the underlying distribution $P_L(f)$ computed here, except for its width, and replaces it by the model-independent function obtained from extreme value statistics. As an illustration, we have plotted the force distribution obtained using Eq. (65) for $M/w=10$ in Fig. 6.

The above arguments suggest that the critical-force distribution computed here via the FRG should be compared with the numerics on a cylinder of aspect ratio parameter $k \approx k_w$ defined above from the width. We now propose a more precise statement to identify the critical force computed in this paper. We note that in the calculations performed here within the FRG the position of the center of mass was held fixed (since all momentum integrations excluded the uniform mode $q=0$). Hence we are working in the *fixed center of mass ensemble*. This suggests the definition

$$f_c(u_0,L) = \max_{\alpha(u_0,L)} \{f_d[\alpha(u_0,L)]\}, \tag{66}$$

where the maximum is over all configurations $\alpha(u_0,L)$ with center of mass u_0 and length L (and periodic boundary conditions along the interface). It can in principle be evaluated numerically by direct enumeration for a discrete interface model. One can then check that it has a well-defined $L \to \infty$ limit with no need for a transverse box, and one can then numerically compute the finite-size distribution for the ensemble of $\alpha(u_0,L)$. This distribution should identify with the one computed here within the FRG (in the massless scheme). It is a more fundamental object than the critical force defined on a cylinder. The latter can then be retrieved in principle as

$$f_c^r = \max_{u_0} f_c(u_0,L) \tag{67}$$

on the same cylinder, leading to extremal statistics, as discussed above.

The above considerations illustrate that the statistics of the depinning threshold force at finite size is a rather subtle question. Many questions remain open. It would be interesting to find the proper steady state corresponding to the above definition (66). Also, a systematic study of memory effects in the threshold force would be of high interest, especially regarding experiments. Indeed, these memory effects may be of importance for aging [36] and hysteresis phenomena [37] controlled in some regimes by the slow dynamics of domain walls. There the observed threshold force may not be the largest one but a threshold force that characterizes a piece of the sample in which that interface got trapped. Hence the data should be interpreted with care to disentangle history effects from finite-size effects. It would be very interesting to develop numerical schemes to investigate these questions, in particular, an efficient algorithm to compute Eq. (66).

ACKNOWLEDGMENTS

We thank O. Duemmer, W. Krauth, and A. Rosso for useful discussions. A.A.F. acknowledges support from the European Commission through Marie Curie Action under Contract No. MIF1-CT-2005-021897. P.L.D. and K.J.W. acknowledge support from ANR program Contract No. 05-BLAN-0099-01.

APPENDIX: CALCULATION OF THE ASYMPTOTICS OF $\Gamma^{(+)}_{\hat{u}\hat{u}u}$

To renormalize the nth cumulant of the critical force we need the leading asymptotics of the vertex functions $\Gamma^{(+)}_{\hat{u}\hat{u}u}$ and $\Gamma^{(-)}_{\hat{u}\hat{u}u}$. The latter is insensitive to the IR cutoff scheme up to corrections to the amplitude. In order to extract this asymptotics, we adopt a massive scheme for the IR regularization because it leads to the simplest calculations. If one then needs the corresponding amplitude in a different scheme, one can relate it to the amplitude in the massive scheme following the methods developed in Ref. [38].

Straightforward perturbation theory gives to first order in the bare disorder denoted here Δ_0 for the "open" vertex $\Gamma^{(+)}_{\hat{u}\hat{u}u}$,

$$\int_{t_2} \Gamma^{(+)}_{\hat{u}\hat{u}u}(t,t_1,t_2;q,-q) = \Delta_0'(0^+)\left\{1 - \Delta_0''(0)\int_p \left[\frac{2}{(p^2+m^2)[(p+q)^2+m^2]} + \frac{1}{(p^2+m^2)^2} + O(e^{-p^2(t-t_1)})\right]\right\}, \tag{A1}$$

$$\int_{t_2} \Gamma^{(-)}_{\hat{u}\hat{u}u}(t,t_1,t_2;q,-q) = -\int_{t_2} \Gamma^{(+)}_{\hat{u}\hat{u}u}(t,t_1,t_2;q,-q). \tag{A2}$$

Identity (A2) holds to all orders by definition. The last term in Eq. (A1) reflects the dynamic nature of the vertex $\Gamma^{(+)}_{\hat{u}\hat{u}u}(t,t_1,t_2;q,-q)$. However, if we integrated this term also over t_1 the result will not depend on the observation time t. As a consequence, the nth cumulant of the critical force is

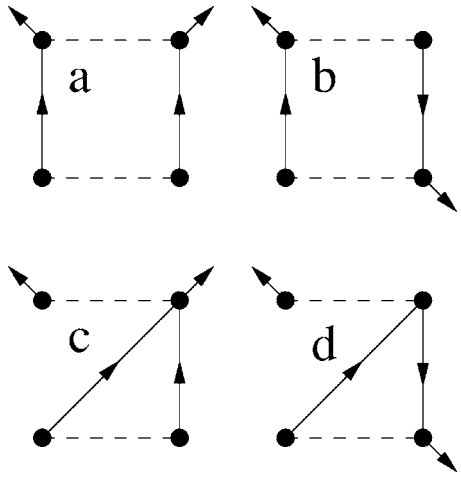

FIG. 7. One-loop dynamical diagrams correcting Δ.

determined by the quasistatic integrals (to any order in disorder).

The easiest way to obtain Eq. (A1) is as follows: One starts from the one-loop diagrams given in Fig. 7, expands to first order in the fields u, and then replaces $\Delta_0^{(n)}(u_t-u_{t'})$ by $\Delta_0^{(n)}(0^+)[\mathrm{sgn}(t-t')]^n$. The diagrams are then split into the two classes $\Gamma^{(-)}_{\hat{u}\hat{u}u}$ and $\Gamma^{(+)}_{\hat{u}\hat{u}u}$, depending on whether the single field u is connected to $\hat{u}(t_1)$ or $\hat{u}(t_2)$. In order to extract the time-independent terms, one chooses $t-t_1\to\infty$. This prescription allows for an easy integration of all 16 diagrams (Refs. [39,40]). Denoting

$$I_1(q)=\int_p \frac{1}{(p^2+m^2)[(p+q)^2+m^2]}=m^{-\varepsilon}\tilde{I}_1(q/m), \tag{A3}$$

and $\tilde{I}_1=\tilde{I}_1(0)$, the contributions to Eq. (A1) are as follows:

$$\begin{aligned}&-\{[I_1(q)]+[I_1(0)+I_1(q)]+[0]+[I_1(0)-I_1(q)]\}\\&\quad\times\Delta_0'(0)\Delta_0''(0)+\{[-I_1(0)]+[0]+[I_1(0)]\\&\quad+[0]\}\Delta_0(0),\Delta_0'''(0),\end{aligned} \tag{A4}$$

where terms in rectangular brackets are in the order of their appearance from diagrams (a), (b), (c), and (d) of Fig. 7. We remark that contributions proportional to $\Delta_0(0)\Delta_0'''(0)$ exactly cancel, and we obtain Eq. (A1).

To renormalize the vertex function (A1) we have to reexpress the bare disorder correlator by the renormalized dimensionless one,

$$\Delta_0(u)=m^{\varepsilon}(\Delta(u)+\{\Delta'(u)^2+[\Delta(u)-\Delta(0)]\Delta''(u)\}\tilde{I}_1).$$

Differentiating the latter expression with respect to u we get after rescaling $\Delta(u)=\frac{1}{\varepsilon\tilde{I}_1}m^{-2\zeta}\tilde{\Delta}(um^{\zeta})$,

$$\Delta_0'(0)=\frac{m^{\varepsilon-\zeta}}{\varepsilon\tilde{I}_1}\tilde{\Delta}'(0^+)\left[1+\frac{3}{\varepsilon\tilde{I}_1}\tilde{\Delta}''(0)m^{\varepsilon}\int_p\frac{1}{(p^2+m^2)^2}\right],$$

$$\Delta_0''(0)=\frac{1}{\varepsilon\tilde{I}_1}m^{\varepsilon}\tilde{\Delta}''(0^+)+O[\tilde{\Delta}''(0)^2,\tilde{\Delta}'(0^+)\tilde{\Delta}'''(0^+)].$$

Omitting the last term in Eq. (A1) we obtain the following expression for the renormalized vertex function:

$$\begin{aligned}&\int_{t_2}\Gamma^{(+)}_{\hat{u}\hat{u}u}(t,t_1,t_2;q,-q)\\&\quad=m^{\varepsilon-\zeta}\frac{1}{\varepsilon\tilde{I}_1}\tilde{\Delta}'(0^+)\left[1-2\tilde{\Delta}''(0)\frac{1}{\varepsilon\tilde{I}_1}m^{\varepsilon}[I_1(q)-I_1(0)]\right].\end{aligned}$$

Note that depinning of the nonperiodic systems is described by the fixed point with $\tilde{\Delta}''(0)^*=\frac{2}{9}\varepsilon+O(\varepsilon^2)$. The one-loop integral $\tilde{I}_1(y)$ reads [17]

$$\tilde{I}_1(y)=\frac{1}{2}K_d\Gamma\left(\frac{d}{2}\right)\Gamma\left(\frac{\varepsilon}{2}\right)\int_0^1\frac{d\alpha}{[1+\alpha(1-\alpha)y^2]^{\varepsilon/2}}, \tag{A5}$$

where $K_d=2\pi^{d/2}/[(2\pi)^d\Gamma(d/2)]$ is the area of a d-dimensional sphere divided by $(2\pi)^d$. Taking into account that $\tilde{I}_1\equiv\tilde{I}_1(0)=\int_q(q^2+1)^{-2}=\frac{1}{2}K_d\Gamma(\frac{d}{2})\Gamma(\frac{\varepsilon}{2})$ we obtain

$$\begin{aligned}&\int_{t_2}\Gamma^{(+)}_{\hat{u}\hat{u}u}(t,t_1,t_2;q,-q)\\&\quad=m^{\varepsilon-\zeta}\frac{1}{\varepsilon\tilde{I}_1}\tilde{\Delta}'^{*}(0^+)\\&\qquad\times\left[1+\frac{2}{9}\varepsilon\int_0^1 d\alpha\ln[1+\alpha(1-\alpha)y^2]+O(\varepsilon^2)\right].\end{aligned}$$

We are interested in the asymptotic behavior for $z\to\infty$. In this limit we have

$$\begin{aligned}&\int_0^1 d\alpha\ln[1+\alpha(1-\alpha)y^2]\\&\quad=-2+\frac{\sqrt{4+y^2}}{y}[\ln 2-\ln(2+y^2-y\sqrt{4+y^2})]\\&\quad=-2+2\ln y+O\left(\frac{\ln y}{y^2}\right).\end{aligned}$$

Matching to a power-law asymptotic behavior we find

$$1+\frac{2}{9}\varepsilon(-2+2\ln y)+O(\varepsilon^2)\to y^{4\varepsilon/9}\left(1-\frac{4}{9}\varepsilon\right). \tag{A6}$$

As a result we obtain for $q/m\gg 1$,

$$\int_{t_2}\Gamma^{(+)}_{\hat{u}\hat{u}u}(t,t_1,t_2;q,-q)=m^{\varepsilon-\zeta}\frac{1}{\varepsilon\tilde{I}_1}\tilde{\Delta}'^{*}(0^+)\left(\frac{q}{m}\right)^{4\varepsilon/9}\left(1-\frac{4}{9}\varepsilon\right). \tag{A7}$$

Replacing m by $1/L$ we obtain Eq. (38).

[1] D. S. Fisher, Phys. Rep. **301**, 113 (1998).
[2] M. Kardar, Phys. Rep. **301**, 85 (1998).
[3] S. Brazovskii and T. Nattermann, Adv. Phys. **53**, 177 (2004).
[4] K. Binder and A. P. Young, Rev. Mod. Phys. **58**, 801 (1986).
[5] D. E. Feldman, Phys. Rev. Lett. **88**, 177202 (2002); P. Le Doussal and K. J. Wiese, *ibid.* **96**, 197202 (2006).
[6] G. Grüner, Rev. Mod. Phys. **60**, 1129 (1988).
[7] G. Blatter, M. V. Feigel'man, V. B. Geshkenbein, A. I. Larkin, and V. M. Vinokur, Rev. Mod. Phys. **66**, 1125 (1994).
[8] T. Giamarchi and P. Le Doussal, Phys. Rev. Lett. **72**, 1530 (1994); Phys. Rev. B **52**, 1242 (1995).
[9] S. Lemerle *et al.*, Phys. Rev. Lett. **80**, 849 (1998).
[10] D. Wilkinsion and J. F. Willemsen, J. Phys. A **16**, 3365 (1983).
[11] S. Zapperi and M. Zaiser, Mater. Sci. Eng., A **309-310**, 348 (2000).
[12] D. S. Fisher, Phys. Rev. B **31**, 1396 (1985).
[13] D. S. Fisher, Phys. Rev. Lett. **56**, 1964 (1986).
[14] T. Nattermann, S. Stepanow, L.-H. Tang, and H. Leschhorn, J. Phys. II **2**, 1483 (1992).
[15] O. Narayan and D. S. Fisher, Phys. Rev. B **48**, 7030 (1993).
[16] P. Chauve, P. Le Doussal, and K. Wiese, Phys. Rev. Lett. **86**, 1785 (2001).
[17] P. Le Doussal, K. J. Wiese, and P. Chauve, Phys. Rev. B **66**, 174201 (2002).
[18] K. P. J. Kytölä, E. T. Seppälä, and M. J. Alava, Europhys. Lett. **62**, 35 (2003).
[19] A. A. Fedorenko and S. Stepanow, Phys. Rev. E **68**, 056115 (2003).
[20] A. Rosso, W. Krauth, P. Le Doussal, J. Vannimenus, and K. J. Wiese, Phys. Rev. E **68**, 036128 (2003).
[21] P. Le Doussal and K. J. Wiese, Phys. Rev. E **68**, 046118 (2003).
[22] B. Drossel and M. Kardar, Phys. Rev. E **52**, 4841 (1995).
[23] P. Chauve, T. Giamarchi, and P. Le Doussal, Phys. Rev. B **62**, 6241 (2000).
[24] L. Balents and P. Le Doussal, Phys. Rev. E **69**, 061107 (2004); Europhys. Lett. **65**, 685 (2004); e-print cond-mat/0312338.
[25] V. M. Vinokur, M. C. Marchetti, and L.-W. Chen, Phys. Rev. Lett. **77**, 1845 (1996).
[26] C. Monthus and T. Garel, Eur. Phys. J. B **48**, 393 (2005); J. Stat. Mech.: Theory Exp. (2005), P12011; e-print cond-mat/0605448.
[27] A. Rosso and W. Krauth, Phys. Rev. Lett. **87**, 187002 (2001); Phys. Rev. E **65**, 025101(R) (2002).
[28] C. J. Bolech and A. Rosso, Phys. Rev. Lett. **93**, 125701 (2004).
[29] J. T. Chayes, L. Chayes, D. S. Fisher, and T. Spencer, Phys. Rev. Lett. **57**, 2999 (1986).
[30] P. Le Doussal and T. Giamarchi, Phys. Rev. B **57**, 11356 (1998).
[31] Note that not taking into account q dependence in $\Gamma^{(+)}_{\hat{u}\hat{u}u}(t,t_1,t_2;q,-q)$ amounts to choosing $\psi=0$ while the ansatz used in the calculation of the width distribution [21], i.e., replacing $q^{-4}\to q^{-d-2\zeta}$, would amount to choosing $\psi=\varepsilon/6$.
[32] O. Duemmer and W. Krauth, Phys. Rev. E **71**, 061601 (2005).
[33] A. Rosso, A. K. Hartmann, and W. Krauth, Phys. Rev. E **67**, 021602 (2003).
[34] A. A. Middleton, Phys. Rev. Lett. **68**, 670 (1992).
[35] J. Galambos, *The Asymptotic Theory of Extreme Order Statistics* (R. E. Krieger Publishing Company, Malabar, Florida, 1987).
[36] E. Vincent, V. Dupuis, M. Alba, J. Hammann, and J.-P. Bouchaud, Europhys. Lett. **50**, 674 (2000).
[37] T. Nattermann, V. Pokrovsky, and V. M. Vinokur, Phys. Rev. Lett. **87**, 197005 (2001); I. F. Lyuksyutov, T. Nattermann, and V. Pokrovsky, Phys. Rev. B **59**, 4260 (1999).
[38] P. Le Doussal, K. J. Wiese, and P. Chauve, Phys. Rev. E **69**, 026112 (2004).
[39] O. Narayan and D. S. Fisher, Phys. Rev. B **46**, 11520 (1992).
[40] T. Antal, M. Droz, G. Györgyi, and Z. Rácz, Phys. Rev. Lett. **87**, 240601 (2001).